INSTITUTE OF PHYSICS PUBLISHING NANOTECHNOLOGY
Nanotechnology **17** (2006) 5406–5411 doi:10.1088/0957-4484/17/21/020

Synthesis of a new type of $GdAl_2$ nanocapsule with a large cryogenic magnetocaloric effect and novel coral-like aggregates self-assembled by nanocapsules

Song Ma, Dianyu Geng, Weishan Zhang, Wei Liu, Xiuliang Ma and Zhidong Zhang

Shenyang National Laboratory for Material Science, Institute of Metal Research, and International Centre for Material Physics, Chinese Academy of Sciences, 72 Wenhua Road, Shenyang 110016, People's Republic of China

E-mail: Songma@imr.ac.cn

Received 18 July 2006, in final form 20 September 2006
Published 13 October 2006
Online at stacks.iop.org/Nano/17/5406

Abstract

A new type of $GdAl_2$ nanocapsule with single-phase intermetallic compound $GdAl_2$ as the core and amorphous Al_2O_3 as the shell has been synthesized by the arc-discharge technique with modified strategies. Meanwhile, novel three-dimensional coral-like hierarchical branching macro-aggregates were self-assembled by disordered nanocapsules synthesized simultaneously in the arc-discharge process. The $GdAl_2$ nanocapsules display superparamagnetic properties between their blocking temperature of 100 K and Curie temperature of 162 K. The magnetocaloric effect of the $GdAl_2$ nanocapsules was measured between 5 and 165 K. The absolute value of the change of magnetic entropy of the $GdAl_2$ nanocapsules sharply increases with decreasing temperature and reaches 14.5 J kg^{-1} K^{-1} at 5 K in magnetic fields varying from 0 to 50 kOe. As a result, this new type of nanocapsule can prospectively be applied in cryogenic magnetic refrigerator devices.

1. Introduction

Recently, interest in research on magnetic nanocapsules has been enhanced considerably because their intermediate states between bulk and atomic materials may present different magnetic behaviours from their correspondent bulk counterparts. This difference offers an opportunity for researchers to investigate the dimensionally confined system in basic research areas and develop many important technical applications, including magnetic refrigerators, magnetic recording, magnetic fluids, catalysts, superconductors and medicine [1]. As the principal contributor of the novel properties, various magnetic cores of nanocapsules, including rare earths and their carbides [2, 3], Fe [4, 5], Co [6, 7], Fe–Co [8, 9], Ni [7, 10, 11], Mn [12], and Co–Cr solid solution [13], have been researched extensively over the past two decades. Apart from single magnetic elements and their carbides, however, cores of compounds need to be exploited to adapt to high-speed developing nanoscience and nanotechnology. Consequently, cores of magnetic rare-earth intermetallic compounds are turning into one of the principal candidates in the field of nanotechnology.

Ferromagnetic intermetallic compounds on the nanoscale will have potential applications in low-temperature magnetic refrigeration because of their superparamagnetic properties. According to theoretical calculation, McMichael concluded that the nanoparticles may exhibit an effective magnetic moment that is greater than the magnetic moment of the constituent atoms, so the magnetic entropy of the nanoparticles may have a maximum enhancement of the magnetocaloric effect (MCE) [14]. Yamamoto *et al* [15, 16] investigated the entropy change in Fe_2O_3–Ag nanocomposites, confirming the prediction of McMichael. Provenzano *et al* [17] reported an MCE of $R_3Ga_{5-x}Fe_xO_{12}$ nanocomposites (R = Gd, Dy and Ho), but the largest ΔS_M is -1.7 J kg^{-1} K^{-1}. Nelson *et al* [18] attempted to prepare Gd nanoparticles in solution, yet

they had considerable difficulties in preventing oxidation of the particles. It is a common fact that it is extremely difficult to synthesize the nanoparticles/nanocapsules with rare-earth elements or compounds because of the chemical activity of the rare earths. Therefore, it is necessary to explore a new type of nanoparticle to acquire larger entropy change and to prevent the magnetic nanoparticles from being oxidized. A new type of superparamagnetic $GdAl_2$ nanocapsule with high atomic moments, low crystalline anisotropy and shell protection would have much more advantages than other nanocomposites for application in cryogenic magnetic refrigerator devices.

During preparation of the nano-products, these nano-units, such as nanoparticles, nanoclusters, nanowires and nanorods, can also self-assemble into the novel structural aggregates through several routes, including electron irradiation deposition [19], chemical vapour deposition [20], laser vaporization–condensation [21], charge transferring [22], an organic reagent-assisted method [23], the solution–liquid–solid method [24] and catalytic vapour–liquid–solid growth [25]. With these routes, various nanoscale or microscale aggregates can demonstrate novel architectures, including tree-like, web-like, spherical, nanowire-like, network and fishbone-like aggregates. As a well-known method for producing the nanocapsules, however, arc-discharge has rarely been used to synthesize the aggregates self-assembled by the nanocapsules prepared simultaneously in arc discharge. Nevertheless, it is possible that arc discharge can be developed into a new way of synthesizing the aggregates.

In the present work, we utilized an arc-discharge technique with modified strategies, involving changing the hydrogen pressure, introducing a gadolinium–aluminium alloy ingot as the anode, and adjusting the proportions of elements in the anode according to their evaporation pressures, to synthesize a new type of nanocapsule, with the intermetallic compound $GdAl_2$ as the core and amorphous Al_2O_3 as the shell, which enlarges the family of magnetic nanocapsules. At the same time, regularly aligned three-dimensional macro-aggregates self-assembled by the nanocapsules without any template and catalyst were simultaneously synthesized in an arc-discharge process.

2. Experiment details

The $GdAl_2$ nanocapsules, which self-assembled into the coral-like aggregates, were synthesized by the well-known arc-discharge method with modified strategies. In the purified argon atmosphere, an anode Gd–Al alloy button was prepared by melting Al and Gd flakes of 99.9 wt% purity at least four times by arc discharge so that the components were homogeneous. The optimum atomic proportions of the button were 80 at.% Gd and 20 at.% Al on the basis of their evaporation pressures. The cathode was a tungsten needle with a diameter of 3 mm. The anode target was placed into one pit of a water-cooled copper crucible. The angle between the anode and the cathode was about 60°. After the chamber was evacuated to 6.6×10^{-3} Pa, argon was introduced into the chamber to reach 0.02 MPa, and then H_2 was introduced into the chamber to reach 0.006 MPa, exceeding the critical value of 0.03 MPa, above which the metal atoms can evaporate rapidly. Then the arc was ignited and the current was maintained at 80 A for 5 h. After being passivated in 0.02 MPa argon for 72 h, large-area black macro-aggregates were collected on the copper crucible in front of the target.

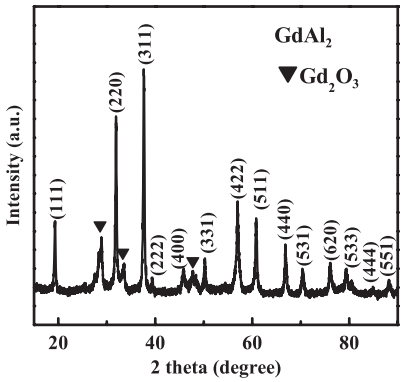

Figure 1. X-ray diffraction (XRD) spectrum of the products.

Phase analysis of the products was performed by powder x-ray diffraction (XRD) on a Rigaku D/max-2000 diffractometer at a voltage of 50 kV and a current of 250 mA with graphite monochromatized Cu Kα ($\lambda = 0.154\,056$ nm). The architecture of aggregates self-assembled by nanocapsules was characterized by a Philips XL-30 scanning electron microscope (SEM), with an emission voltage of 20 kV. The detailed morphology of the corresponding nanocapsules was examined by means of high-resolution transmission electron microscopy (HRTEM) using a JEOL 2010 and Tecnai G^2 F30 with emission voltages of 200 and 300 kV, respectively. X-ray photoelectron spectroscopy (XPS) measurements were performed on an ESCALAB-250 with a monochromatic x-ray source (an aluminium Kα line of 1486.6 eV energy and 150 W) to characterize the valence of surface Al atoms of the nanocapsules at a depth of 1.6 nm. The magnetic properties of the nanocapsules were measured on a Quantum Design MPMS-7 superconducting quantum interference device (SQUID).

3. Result and discussion

The XRD pattern clearly shows the phase composition of the as-prepared products in figure 1. In addition to several peaks indicating the existence of a small amount of Gd_2O_3, most sharp reflection peaks could be indexed to the single-phase intermetallic compound $GdAl_2$. The formation of these phases is due to the bumping of the metal atoms evaporating from the molten pool of the anode [26]. It is noteworthy that only $GdAl_2$ binary compound appears in the present products and that no other intermetallic compounds in the Gd–Al binary system are found in the XRD pattern. The facts that Gd and Al atoms are of appropriate proportions and that the $GdAl_2$ is a stable phase with the highest decomposition temperature in the Gd–Al phase diagram play important roles in the formation of single-phase $GdAl_2$. When the composition of the anode is changed, Gd_3Al_2 can be found in the products, indicating the importance of appropriate atomic proportions of the two different metals. In the arc-discharge process, a small number of gadolinium particles formed by excessive gadolinium atoms were oxidized into Gd_2O_3 when exposed to the air.

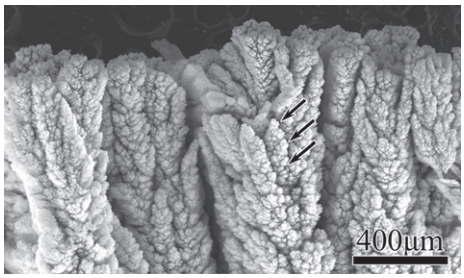

Figure 2. Low-magnification SEM image of the upper part of the aggregate arrays and one of the big branches in an aggregate indicated by arrows.

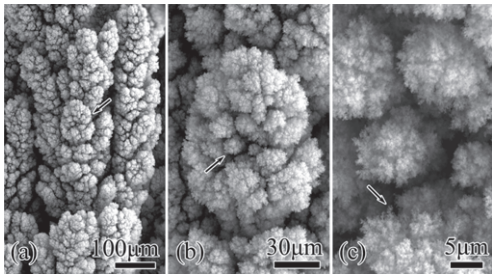

Figure 3. Typical SEM images of the middle part of the aggregates. (a) The architecture of aggregates built up by rod-like branches. (b) One big cluster in the rod branch indicated by the arrow in (a) and one small cluster indicated by the arrow. (c) Small clusters building up the big clusters and flocculent structure indicated by the arrow.

3.1. Structural analysis of the aggregates

The morphology of the upper part of the aggregates was examined by scanning electron microscopy (SEM), as is shown in figure 2. A low-magnification SEM image reveals that every aggregate displays coral-like architecture with hierarchical branching characteristics along the axial and lengthwise directions, and the average diameter ranges from 100 to 200 μm. Large branches of aggregates with a length of about 200 μm and a width of 50 μm closely arrange from inside to outside. The distance between two aggregates is kept to about 50 μm, which indicates that each aggregate grew separately.

A typical SEM image of the middle part of an aggregate is shown in figure 3 at different magnification. The morphology of the aggregates indicates their growth characteristics in the arc-discharge process. Obviously, the rod-like big branches locate in the space built up by under-floor branches and the same floor branches are almost of the same height. Accordingly, it can be concluded that the big branches around the main stem of aggregates grew separately and constructed the space for the growth of upside floor branches simultaneously. It can be observed from figures 3(a) and (b) that a big branch comprises some big clusters and a big cluster also consists of many small irregular spherical clusters, with diameter distribution from 5 to 10 μm, stacking together and keeping a distance of about 2 μm. The SEM image at a high magnification shows the clear morphology of small clusters (figure 3(c)), which are composed of flocculent structure formed by the small particles adhering together. The existence of the distance between clusters and big branches can be explained by the fact that they carried the redundant negative charge from the plasma to repulse each other [19].

In figure 4, the root of an aggregate is clearly shown. The diameter of the root is about 80 μm, smaller than the middle and upper parts of the aggregates (figure 4(a)). The local morphology of the root shows that big clusters with a diameter of about 40 μm congregate together to construct the root (figure 4(b)). A higher-magnification SEM image of the root shows that the flocculent structures array like a lawn along the same direction (figure 4(c)). A high-magnification SEM image of a flocculent structure is shown clearly in figure 4(d), in which the particles adhere together to form line-like flocculent structures. These characteristics indicate that the flocculent structures directly constructed the roots of the aggregates or adhered together to form big clusters on the roots of aggregates,

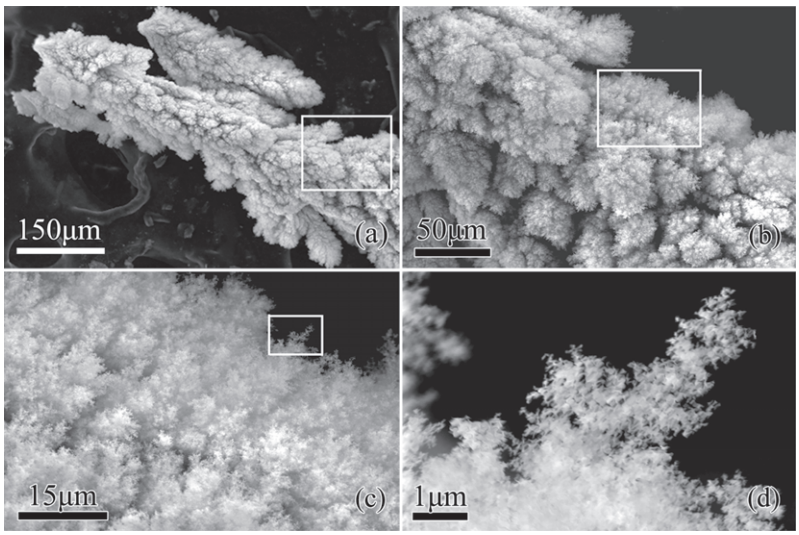

Figure 4. Different magnification SEM images of the root of aggregates indicating (a) the morphology of the root, (b) a local image of the aggregates in the frame of (a), (c) flocculent structure arrays in the frame of (b), and (d) particles adhering together to form the flocculent structure in the frame in (c).

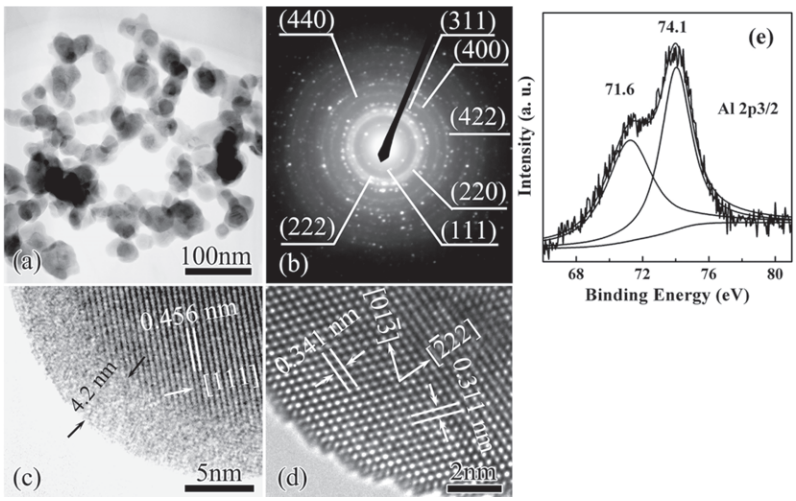

Figure 5. (a) The diameter distribution of the nanocapsules. (b) The SAD pattern of the two particles. (c) HRTEM image of the $GdAl_2$ nanocapsules. (d) HRTEM image of Gd_2O_3 nanoparticles. (e) XPS spectrum and corresponding fitting curve of the Al atoms at a depth of 1.6 nm of the nanocapsules.

because the flocculent structures carrying negative charge from the plasma are more easily attracted to the surface of the anode to form roots at the initial stage of the arc-discharge process.

3.2. Structure of the nanocapsules

The morphology of the nanocapsules constructing the aggregates was examined from the low-magnification TEM images (figure 5(a)). The particles are of irregular spherical shape or a strip with curvature, and the diameter distribution is 20–50 nm, which makes it easy for them to adhere together to form a flocculent structure. From the selected area electron diffraction (SAED) pattern, $GdAl_2$ and Gd_2O_3 can be determined from the characteristic diffraction rings, indicating the characteristic lattice planes (111), (220), (311), (400) and (422) of $GdAl_2$ and (222) and (440) of Gd_2O_3, respectively (figure 5(b)), which is consistent with the results of the XRD pattern. In figure 5(c), the HRTEM image clearly shows the shell/core structure with a crystalline core and an amorphous shell 4.2 nm thick. In the core, the *d*-spacing of 0.456 nm corresponds to the lattice fringe {111} of $GdAl_2$. An HRTEM image of the nanoparticle, without a shell/core structure (figure 5(d)), shows the characteristic lattice fringes' {222} plane and {013} plane with *d*-spacings of 0.311 and 0.341 nm respectively, which corresponds to Gd_2O_3. The shell of the nanocapsules can be determined as Al_2O_3 from the binding energy peak of 74.1 eV [27], which is shown in the XPS spectrum with an etching depth of 1.6 nm (figure 5(e)). Another binding energy peak of 71.6 eV of Al2p3/2 represents the compound $GdAl_2$ [27], the intensity of which is lower than that of Al_2O_3, indicating the existence of some nanocapsules with a shell thinner than 1.6 nm. The formation of an Al_2O_3 shell was explained by the fact that Al atoms with higher velocities, due to smaller atomic mass, were more easily absorbed on the outside of the $GdAl_2$ nanoparticles and subsequently condensed on the surface. When the products were exposed to air, Al atoms were easily oxidized to amorphous Al_2O_3 [26].

3.3. Magnetic properties and MCE of the nanocapsules

The zero-field-cooled and field-cooled (ZFC–FC) curves of the $GdAl_2$ nanocapsules were measured from 5 to 300 K at an applied field of 100 Oe. From figure 6(a), it can be clearly observed that a peak of the ZFC curve appears at 100 K, indicating the blocking temperature T_B, and the bifurcation between ZFC and FC curves appears. Furthermore, the peaks in the temperature dependence of ac susceptibility (in the inset of figure 6(a)) do not shift their positions with an increase in frequency from 10 to 1000 Hz, which is different from the character of the spin-glass-like state in which the peaks would shift to lower temperatures with increasing frequency. A pivotal point at 162 K in the two overlapping curves indicates the Curie temperature T_C of $GdAl_2$ nanocapsules, which is slightly lower than 172 K for the bulk counterpart because of the dimensional effect [1]. It can be concluded that $GdAl_2$ nanocapsules are of a superparamagnetic property between the blocking temperature T_B and the Curie temperature T_C, because their sizes are decreased to the nanoscale. From the magnetic hysteresis loops in figure 6(b), the coercive force at 5 K is 280 Oe, showing their ferromagnetic behaviour at low temperatures. The magnetization at 180 K increases linearly with the increase in the magnetic field, indicating their paramagnetism. Because the only phase components in the nanocapsules are ferromagnetic $GdAl_2$ and paramagnetic Gd_2O_3, this may exclude the contribution of antiferromagnetic components to magnetization at low temperatures.

By grouping spins together in superparamagnetic $GdAl_2$ nanocapsules, the magnetic moments are more easily aligned than in the paramagnetic system for certain ranges of field at low temperature, and the entropy of the spins is more easily changed by the application of a field. According to the experimental results of Yamamoto *et al* [15, 16], the isothermal magnetic entropy change around 250 K in 9% Fe of Fe_2O_3–Ag nanocomposite reached about 2.1×10^{-3} J mol^{-1}(Fe) in a magnetic field varying from 0 to 70 kOe, which exceeded that of normal paramagnetic Fe^{3+} in the same temperature and magnetic field range by about two orders of magnitude.

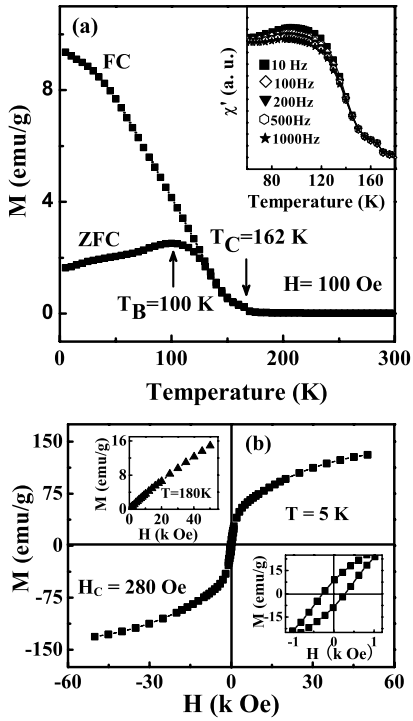

Figure 6. (a) Zero-field-cooled and field-cooled ($H = 100$ Oe) magnetization curve of the nanocapsules; the inset is the temperature dependence of ac susceptibility with frequencies from 10 to 1000 Hz. (b) Magnetic hysteresis loop at 5 K; the insets are, respectively, the magnetic field dependence of magnetization at 180 K and the low-field part of the hysteresis loop at 5 K.

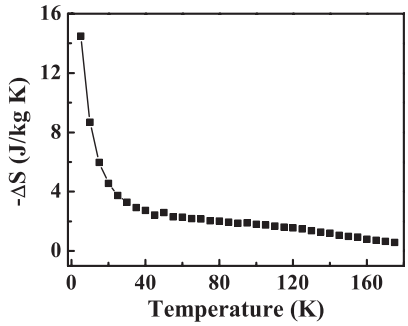

Figure 7. The change in magnetic entropy of $GdAl_2$ nanocapsules between 5 and 165 K in an applied field varying from 0 to 50 kOe.

However, the extensive measure of the MCE is reduced by a factor proportional to the ratio of the volumes (or the mass) of the inactive matrix [28]. In the magnetic cores of the present nanocapsules, the total angular momentum of the Gd atom is $J = 7/2$ and its effective magnetic moment is 7.2 μ_B. So $GdAl_2$ nanocapsules will have large magnetization, ensuring that more spins contribute to the entropy change. On the other hand, the lower crystalline anisotropy [29] of $GdAl_2$ will make the moments of particles align easily along the applied field. It is also worth noting that the Al_2O_3 shell of nanocapsules can prevent the $GdAl_2$ cores from being oxidized and interacting with each other. In view of the advantages mentioned above, the change in entropy in the $GdAl_2$ nanocapsules was measured from 5 to 165 K in a magnetic field varying from 0 to 50 kOe. At low temperatures, the absolute ΔS_M value sharply increases with a decrease in temperature and reaches 14.5 J kg^{-1} K^{-1} at 5 K (figure 7). Delightfully, not only the $GdAl_2$ nanocapsules with large entropy change at low temperatures will have potential applications in the future, but also the strategy of preparation of $GdAl_2$ nanocapsules will open up a new route for preparing more compounds of magnetic nanocapsules.

4. Conclusion

Using an arc-discharge technique with a modified strategy, nanocapsules with a single-phase $GdAl_2$ core were fabricated and three-dimensional coral-like macro-aggregates were self-assembled by the new type of $GdAl_2$ nanocapsules simultaneously. The phase compositions of the product were determined as single-phase $GdAl_2$ and a small amount of Gd_2O_3 from XRD and TEM measurements. Using SEM, the architecture of the hierarchical branching aggregates was shown to be constructed from nanocapsules, flocculent structure, small clusters, big clusters and big branches step by step at different scales, which indicates the self-similar attributes of the structure. The $GdAl_2$ nanocapsules have a shell/core structure with crystalline $GdAl_2$ as the core and amorphous Al_2O_3 as the shell, respectively. The new type of $GdAl_2$ nanocapsules shows superparamagnetic properties between their blocking temperature of 100 K and Curie temperature of 162 K. The $GdAl_2$ nanocapsules show ferromagnetic behaviour at low temperatures. The peaks in the temperature dependence of ac susceptibility do not shift their positions with an increase in frequency from 10 to 1000 Hz, which excludes the possibility of the existence of a spin–glass-like state. On the other hand, the only phase components in the nanocapsules are ferromagnetic $GdAl_2$ and paramagnetic Gd_2O_3, which excludes possible contributions of the antiferromagnetic components at low temperature. The absolute value of the change in magnetic entropy sharply increases with an decrease in temperature at low temperature and reaches 14.5 J kg^{-1} K^{-1} at 5 K. Consequently, $GdAl_2$ nanocapsules can be applied as a promising MCE material for low-temperature MCE devices. At the same time, the present strategy using an arc-discharge technique opens up a new way of synthesizing more magnetic nanocapsules of rare-earth compounds.

Acknowledgments

This work was supported by the National Natural Science Foundation of China under grant no. 50331030. The authors thank Dr W F Li for helpful discussions.

References

[1] Zhang Z D 2004 *Nanocapsules* (*Encyclopedia of Nanoscience and Nanotechnology* vol 6) ed H S Nalwa (California: American Scientific) pp 77–160
[2] Saito Y, Okuda M, Yoshikawa T, Kasuya A and Nishina Y 1994 *J. Phys. Chem.* **98** 6696
[3] Ruoff R S, Lorents D C, Chan B, Malhotra R and Subramoney S 1993 *Science* **259** 346
[4] Sun X C and Nava N 2002 *Nano Lett.* **2** 765
[5] Fernandez-Pacheco R, Arruebo M, Marquina C, Ibarra R, Arbiol J and Santamaria J 2006 *Nanotechnology* **17** 1188
[6] Saito Y 1995 *Carbon* **33** 979

[7] Liu Y, Ling J, Wei U and Zhang X G 2004 *Nanotechnology* **15** 43
[8] Dong X L, Zhang Z D, Chuang Y C and Jin S R 1999 *Phys. Rev.* B **60** 3017
[9] Pozas R, Ocana M, Morales M P, Tartaj P, Nunez N and Serna C J 2004 *Nanotechnology* **15** S190
[10] Si P Z, Zhang Z D, Geng D Y, You C Y, Zhao X G and Zhang W S 2003 *Carbon* **41** 247
[11] Ang K H, Alexandrou I, Mathur N D, Amaratunga G A J and Haq S 2004 *Nanotechnology* **15** 520
[12] Si P Z, Li D, Lee J W, Choi C J, Zhang Z D, Geng D Y and Bruck E 2005 *Appl. Phys. Lett.* **87** 133122
[13] Ma S, Wang Y B, Geng D Y, Li J and Zhang Z D 2005 *J. Appl. Phys.* **98** 094304
[14] McMichael R D, Shull R D, Swartzendruber L J and Bennett L H 1992 *J. Magn. Magn. Mater.* **111** 29
[15] Yamamoto T A, Tanaka M, Nakayama T, Nishimaki K, Nakagawa T, Katsura M and Niihara K 2000 *Japan. J. Appl. Phys.* **39** 4761
[16] Yamamoto T A, Tanaka M, Shiomi K, Nakayama T, Nishimaki K, Nakagawa T, Numazawa T, Katsura M and Niihara K 2000 *Mater. Res. Soc. Symp. Proc.* **581** 297
[17] Provenzano V, Li J, King T, Canavan E, Shirron P, Dipirro M and Shull R D 2003 *J. Magn. Magn. Mater.* **266** 185
[18] Nelson J A, Bennett L H and Wagner M J 2002 *J. Am. Chem. Soc.* **124** 2979
[19] Cho S O, Lee E J, Lee H M, Kim J G and Kim Y J 2006 *Adv. Mater.* **18** 60
[20] Dick K A, Deppert K, Larsson M W, Martensson T, Seifert W, Wallenberg L R and Samuelson L 2004 *Nat. Mater.* **3** 380
[21] ElShall M S, Li S T, Graiver D and Pernisz U 1996 Synthesis of nanostructured materials using a laser vaporization-condensation technique *Nanotechnology* (*ACS Symposium Series*) vol 622 pp 79–99
[22] Naka K, Roh H and Chujo Y 2003 *Langmuir* **19** 5496
[23] Lu Q Y, Gao F and Zhao D Y 2002 *Nanotechnology* **13** 741
[24] Boal A K, Ilhan F, Derouchey J E, Thurn-Albrecht T, Russell T P and Rotello V M 2000 *Nature* **404** 6779
[25] Zhu Y Q, Hsu W K, Zhou W Z, Terrones M, Kroto H W and Walton D R M 2001 *Chem. Phys. Lett.* **347** 337
[26] Geng D Y, Zhang Z D, Zhang W S, Si P Z, Zhao X G, Liu W, Hu K Y, Jin Z X and Song X P 2003 *Scr. Mater.* **48** 593
[27] Moulder J F, Stickle W F, Sobol P E and Bomben K D 1992 *Physical Electronics Division* (*Handbook of X-ray Photoelectron Spectroscopy*) ed J Chastain (Minnesota: Perkin-Elmer) p 55
[28] Gschneidner K A Jr, Pecharsky V K and Tsokol A O 2005 *Rep. Prog. Phys.* **68** 1479
[29] Morales M A, Williams D S, Shand P M, Stark C, Pekarek T M, Yue L P, Petkov V and Leslie-Pelecky D L 2004 *Phys. Rev.* B **70** 184407